



## Mixture Model for a Parametric Study on Turbulent Convective Heat Transfer of Water-Al<sub>2</sub>O<sub>3</sub> Nanofluid

Suaib Al Mahmud<sup>1</sup>, Ahmad Faris Ismail<sup>1,\*</sup>, Jamirul Habib Bappy<sup>1</sup>, Wazed Ibne Noor<sup>2</sup>

<sup>1</sup> Department of Mechanical Engineering, Kulliyah of Engineering, International Islamic University Malaysia, 53100 Gombak, Kuala Lumpur, Malaysia

<sup>2</sup> Department of Mechatronics Engineering, Kulliyah of Engineering, International Islamic University Malaysia, 53100 Gombak, Kuala Lumpur, Malaysia

### ARTICLE INFO

#### Article history:

Received 26 December 2021

Received in revised form 7 January 2022

Accepted 9 January 2022

Available online 24 February 2022

#### Keywords:

Nanofluid; forced convection; multiphase; heat transfer; mixture model; parametric

### ABSTRACT

Nanofluids have become a point of intense interest for its usability in sectors where convective heat transfer is a requirement. Whereas knowing the overall thermal transport characteristics of nanofluids is the key for their proper utilisation, the domain of nanofluids turbulent convective heat transfer is still heavily understudied, where conducting a parametric study on their heat transferring behaviour along with assessing the effect of boundary conditions on their heat transfer enhancement and the available CFD models' efficiency to account for nanoparticle size are vital necessities. In this study, highly turbulent flow of nanofluids inside a circular pipe under constant wall temperature has been simulated using the Mixture model. Correlations between all the parameters related to nanofluids turbulent convective heat transfer have been established and the impact of variable temperature boundary condition on nanofluids heat transfer enhancement has been investigated. In addition, Mixture models' ability to assess nanoparticle size variation on heat transfer of nanofluids has been shown. Results suggest that nanofluids heat transfer is dominated by the amount of nanoparticle concentration present in the base fluid when Reynolds number is kept constant. Also, for a certain particle concentration, intensification of heat transfer is guided by the degree of turbulence. The findings also depict that nanofluids heat transferring capability is independent of the temperature boundary conditions used and Mixture model is unable to assess the change in heat transfer due to variation in nanoparticle size.

## 1. Introduction

Nanofluids were discovered as the necessity for efficient heat transferring fluid (HTF) raised in order to ensure satisfactory operation of machines and devices that work based on the principles of heat transfer. Since nanofluids were discovered by Sreelakshmy *et al.*, [1] as a result of introducing nanoscale metallic particles and carbon nanotubes as nanoparticles in heat transferring fluids, a great amount of experimental and numerical studies has been carried out on them. Since a long time now,

\*Corresponding author.

E-mail address: [faris@iium.edu.my](mailto:faris@iium.edu.my) (Ahmad Faris Ismail)

researchers have been trying to understand nanofluids heat transferring behavior by conducting experimental and numerical studies. Though for the numerical studies a lot of studies depended upon single phase CFD model, numerous researchers concluded multiphase CFD models to be performing better in terms of simulating nanofluids heat transfer.

Hanafizadeh *et al.*, [2] examined and compared the multiphase models in terms of predicting heat transfer and found out that at low Reynolds number and developing region of the flow, Mixture model performs better heat transfer coefficient prediction than other models. The study of Lotfi *et al.*, [3] on numerical study of forced convective heat transfer of nanofluids found out that two phase Eulerian model underestimates the Nusselt number. He also concluded mixture model to be more convincing. Meanwhile, Davarnejad and Jamshidzadeh [4] observed that among three multiphase models (VOF, Eulerian and Mixture) VOF and Mixture model predicted friction factor and Nusselt number dramatically. This is quite apparent that among the multiphase models, mixture model seems to be more reliable than the other ones.

Beyond the argument of multiphase models for nanofluids heat transfer simulation, some conclusions have been made on heat transferring behavior of nanofluids by conducting a few parametric studies. In parametric representation of Fard *et al.*, [5] experiment it was found that the coefficient of heat transfer increases with the increase of particle concentration of nanofluid and the heat transfer enhancement keeps increasing with nanofluid's Peclet number. Kriby *et al.*, [6] noticed hike in heat transfer and shear stress due to nanoparticle concentration by which the radial distribution of temperature and velocity is influenced. Lotfi *et al.*, [3] picked up a slightly conflicting conclusion that as nanoparticles volume fraction increases the thermal enhancement rate significantly decreases. The research of Bianco *et al.*, [7] suggests heat transfer enhancement keeps increasing with the hike in volume concentration of particles and Reynolds number. For several volume fraction of nanofluids Davarnejad and Jamshidzadeh [4] found out that, Nusselt number raises with increase in volume fraction of nanoparticles and that aligns with experimental data while a range of Reynolds number were used. Nu and friction factor increased with nanofluid concentration increment. The research of Esfandiary *et al.*, [8] has similar findings with the findings of Bianco *et al.*, [7] in terms of heat transfer. It also concluded that though coefficient of friction remains unaffected with the rise of volume fraction, it decreases as Reynolds number increases. Furthermore, for the flow of nanofluids in a 3-D curved microtube, Akbari *et al.*, [9] found out that nanofluids heat transfer behaves differently near a curvature. They stated that, though near 45-degree curvature increase in nanoparticles volume fraction causes a decrease in friction factor and Nusselt number, in the entrance region the hike in Richardson number and nanoparticle concentration affects the heat transfer and friction factor in opposite manner. Via employment of mixture model for investigation on the effects heterogenous distribution of nanoparticles in heat transfer of nanofluids, Amani *et al.*, [10] discovered that at lower Reynolds number nanoparticle concentration effect on Nusselt number is comparatively more noticeable. In a laminar forced convection study with the same nanofluid in an automotive cooling system it was concluded that friction factor decreases with increased flowrate and increases with hike in nanoparticle volume concentration whereas Nusselt number increases with increase in flowrate, volume concentration and inlet temperature [11]. In another study with water-CuO nanofluid, Parvin *et al.*, [12] found proportional relationship between Prandtl number and laminar convective heat transfer enhancement.

This is known that when the particle concentration is kept constant, the amount of convective heat transfer depends upon the Reynolds number. Some experimental and a few numerical studies have been conducted keeping the particle concentration and Reynolds number constant and by varying the nanoparticle size in order to assess which particle size yields the highest amount of heat transfer. Anoop *et al.*, [13] tried two different particle size for laminar convective heat transfer of

water- $\text{Al}_2\text{O}_3$  nanofluid and found out that smaller nanoparticle size causes higher heat transfer coefficient. Another experimental study of Zhang *et al.*, [14] with water- $\text{SiO}_2$  nanofluid with three different particle sizes showed similar results. Meanwhile, the size dependent study by Angayarkanni *et al.*, [15] on multiple nanofluids suggests that specific heat capacity is inversely proportional to the nanoparticle size of nanofluids. However, the review by Khatke *et al.*, [16] on nanoparticle size on heat transfer augmentation finds a slightly different conclusions and suggests that for  $\text{SiO}_2$  nanofluid, heat transfer coefficient increases with increasing particle size whereas it decreases for  $\text{Al}_2\text{O}_3$  nanofluids as particle size gets bigger. Via a three-dimensional numerical study with  $\text{CuO}/\text{Water}$  nanofluid, Du *et al.*, [17] suggested 40nm to be the optimal particle size for heat transfer and advised to ignore particle size of 5nm and 50nm due to their performance incapability. Another numerical study by Azimi *et al.*, [18] found out that increasing particle size decreases the heat transfer coefficient for fully developed laminar flow of water- $\text{Al}_2\text{O}_3$  nanofluid. By a single phase CFD simulation Davarnejad *et al.*, [19] concluded that smaller nanoparticles give higher heat transfer coefficient for developed region of laminar flow of water- $\text{Al}_2\text{O}_3$  nanofluid.

Whereas a huge amount of concentration has been given to the relationship between nanoparticles volume fraction and Nusselt number, detailed information on relationships among other turbulent convective heat transfer parameters such as Stanton number, Prandlt number, thermal entry length etc. are still missing. In addition, some findings by different researchers contradict with each other. Besides, though a lot of experimental and a few numerical studies were carried out to investigate the effect of particle size on heat transfer enhancement of nanofluids, it has not been investigated yet how multiphase CFD models assesses the particle size effect on nanofluids heat transfer, more precisely how the mixture model does it as this model is the most depended upon multiphase CFD model to simulate nanofluids flow. Apparently, the parametric relationships on nanofluids turbulent forced convective heat transfer are heavily understudied so is the effect of temperature boundary conditions on their heat transfer enhancement. In addition, how the Mixture model assesses the impact of nanoparticle size on nanofluids heat transfer intensification needs to be investigated extensively. Which is why conducting a study demonstrating the relationships between all the necessary variables related to convective heat transfer of nanofluids is essential so that a complete insight on nanofluids heat transferring behavior is gained. In this study highly turbulent flow of water- $\text{Al}_2\text{O}_3$  nanofluid inside a circular pipe under constant wall temperature has been simulated by varying the particle concentration using the Mixture model in order to investigate the overall turbulent convective heat transferring behavior of nanofluids by a detailed parametric investigation and to assess how the mixture model treats the particle size variation in terms of heat transfer enhancement by nanofluids. This study also assess how nanofluids heat transfer is affected by different boundary conditions. This paper is the continuation of the authors another paper on comparison between Mixture and VOF model for convective heat transfer of water- $\text{Al}_2\text{O}_3$  nanofluid [20].

## 2. Governing Equations

The principal equations of fluid dynamics are applicable for the flow of nanofluid where the first equation is the continuity equation demonstrating the conservation of mass, second one is momentum equation representing conservation of momentum and the third one is energy equation that talks about conservation of energy.

## 2.1 Continuity Equation

According to this equation, the rate of mass entering the system exactly equals the rate of mass exiting the system plus the aggregation of mass in the system. The continuity equation for nanoparticles and base fluid can be represented as [5]:

$$\frac{\partial}{\partial t} (\varphi_{\alpha} \rho_{\alpha}) + \nabla \cdot (\varphi_{\alpha} \rho_{\alpha} U_{\alpha} - \Gamma_{\alpha} \nabla \varphi_{\alpha}) = 0 \quad (1)$$

Here,  $\varphi$ ,  $\rho$ ,  $U$  and  $\Gamma$  stand for volume fraction, density, interstitial velocity vector and dispersion coefficient. The subscript  $\alpha$  represents phase index.

## 2.2 Momentum Equation

The momentum equation which is also called Navier-Stokes equation refers to Newton's Second Law relating the rate of momentum change to the number total of forces that act on a component of liquid. The differential form of this equation is as following [5]:

$$\frac{\partial}{\partial t} (\varphi_{\alpha} \rho_{\alpha} U_{\alpha}) + \{ \varphi_{\alpha} [\rho_{\alpha} U_{\alpha} U_{\alpha} - \mu_{e\alpha} (\nabla U_{\alpha} + (\nabla U_{\alpha})^T)] \} = \varphi_{\alpha} (B_{\alpha} - \nabla P) + F_{\alpha} \quad (2)$$

$T$ ,  $B$ ,  $\nabla P$  and  $F$  indicate temperature, body force, pressure drop and interphase force respectively.

## 2.3 Energy Equation

The last equation is about the conservation of energy which states that energy cannot be created or destroyed and it only changes from one form to another. The final amount of energy in a system is same as the previous amount of it but just in a different form. In an equational manner it is represented as [5]:

$$\frac{\partial}{\partial t} (\varphi_{\alpha} \rho_{\alpha} U_{\alpha}) + \nabla \cdot [ \varphi_{\alpha} (\rho_{\alpha} U_{\alpha} h_{\alpha} - k_{\alpha} \nabla T_{\alpha}) ] = \sum_{\beta=1}^N (\Gamma_{\alpha\beta} + h_{\beta s} - \Gamma_{\beta\alpha} h_{\alpha s}) + Q_{\alpha} + S_{\alpha} \quad (3)$$

In this equation, enthalpy, thermal conductivity, interphase heat transfer and external heat source in energy equation are denoted by  $h$ ,  $k$ ,  $Q$  and  $S$ , whereas the subscripts  $\beta$  and  $s$  indicate phase index and solid particles.

## 3. Geometry and Meshing

The geometry considered for this study is a circular pipe with a diameter of 10 mm having a length of 1m that is placed horizontally with respect to the ground (as seen in Figure 1). The geometry was derived from benchmark research paper Bianco *et al.*, [21].

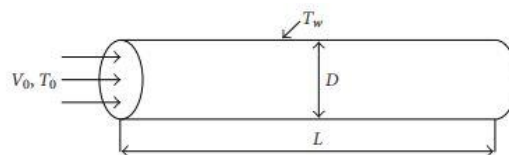
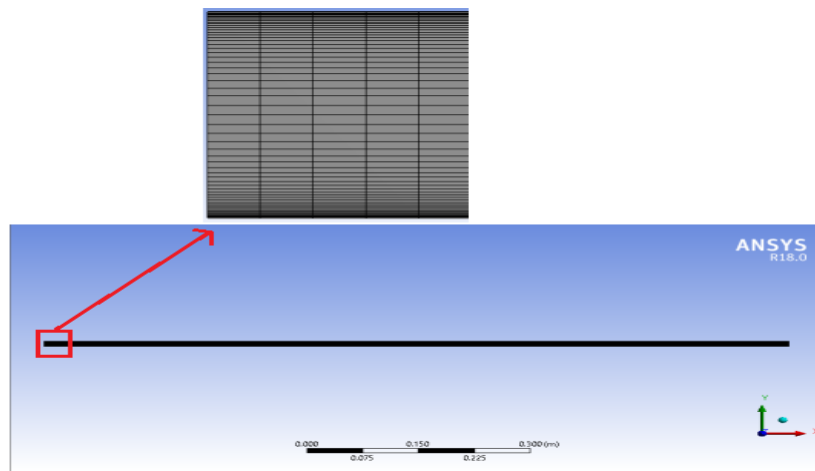


Fig. 1. Geometry for numerical simulation

Geometry specifications are mentioned in Table 1 as following:

Specification	Magnitude
Material	Aluminium
Diameter (mm)	10
Length(mm)	1000
Heat transfer flow area (mm <sup>2</sup> )	31416
Cross sectional area (mm <sup>2</sup> )	78.54
Reynolds number range	20000 - 80000

One of the most important parts of CFD simulation is to create a proper mesh for the simulation. Whereas dense meshing is preferred for statistical reliability and higher precision, a mesh denser than necessary can affect the results of CFD simulation in adverse manner. On a created 2D geometry o the pipe orthogonal structured mesh was created. The mesh was made denser at the near wall region to account for the boundary layers. Mesh created on the geometry for simulation and the Fluent grid close up are represented by Figure 2 and Figure 3 respectively.



**Fig. 2.** Created mesh on 2D pipe geometry

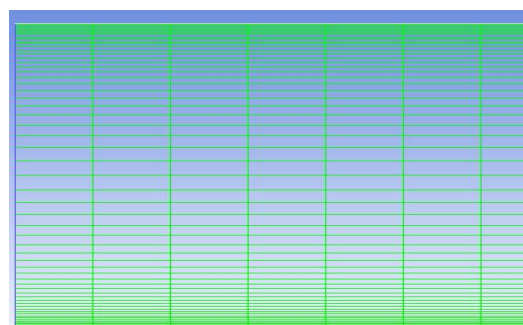


**Fig. 3.** Grid for simulation in Fluent

#### 4. Turbulence Modelling

The realizable  $k-\epsilon$  turbulence model has been considered to simulate the turbulent flow of nanofluid. This model accounts for the turbulent kinetic energy denoted by  $k$  and its dissipation rate which is denoted by  $\epsilon$ . They are described as [22]

$$\frac{\partial}{\partial t} (\rho k) + \frac{\partial}{\partial x_j} (\rho k u_j) = \frac{\partial}{\partial x_j} \left[ \left( \mu + \frac{\mu_t}{\sigma_k} \right) \frac{\partial k}{\partial x_j} \right] + G_k + G_b - \rho \varepsilon - Y_M + S_k \quad (4)$$

$$\frac{\partial}{\partial t} (\rho \varepsilon) + \frac{\partial}{\partial x_j} (\rho \varepsilon u_j) = \frac{\partial}{\partial x_j} \left[ \left( \mu + \frac{\mu_t}{\sigma_\varepsilon} \right) \frac{\partial \varepsilon}{\partial x_j} \right] + \rho C_{1\varepsilon} S_\varepsilon - \rho C_2 \frac{\varepsilon^2}{k + \sqrt{\nu \varepsilon}} + C_{1\varepsilon} \frac{\varepsilon}{k} C_{3\varepsilon} G_b + S_\varepsilon \quad (5)$$

$$C_1 = \max \left[ 0.43, \frac{\eta}{\eta + 5} \right] \quad (6)$$

$$\eta = \sqrt{2 S_i S_j} \frac{k}{\varepsilon} \quad (7)$$

where,  $G_k$  is generation of turbulent kinetic energy because of mean velocity gradients,  $G_b$  represents the generation of turbulence kinetic energy due to buoyancy,  $Y_M$  represents the contribution of the fluctuating dilatation in compressible turbulence to the overall dissipation rate.  $C_2$  and  $C_{1\varepsilon}$  are constants and turbulent Prandtl numbers are represented by  $\sigma_k$  and  $\sigma_\varepsilon$  whereas  $S_k$  and  $S_\varepsilon$  are user defined terms.

## 5. Boundary Conditions

The boundary conditions necessary for the CFD simulation have been picked up from the benchmark paper [21]. The necessary thermophysical properties of the nanofluid have been calculated using the formular provided in that paper. The properties of nanoparticles and the base fluid were obtained from there as well. Table 2 represents the imposed boundary conditions on the geometry for the flow.

**Table 2**  
Boundary conditions used for the simulation

Zone	Nature	Condition imposed
Inlet	Velocity inlet	- Uniform velocity, $V_o$ - Uniform temperature, $T_o = 293$ K
Outlet	Pressure outlet	Gauge pressure = 0 pa
Walls	-	- No slip conditions - Constant temperature $T_w = 350$ K

## 6. Mesh Independence Study (MIS)

The mesh independence test is an important stage in CFD simulation. Given that the accuracy of CFD simulation results is determined by the quality of the mesh, the ideal mesh must be built in such a manner that the output parameter does not vary significantly when the mesh is adjusted.

For this simulation mesh was created in the 2D geometry by creating two edge sizing along the vertical and horizontal edges. The mesh independence study was done by taking outlet average temperature as the output parameter when the number of divisions at the inlet was varied hence the nodes, elements and cell numbers were varied as well. Structured mesh was obtained using face meshing. Biasing method was used for making the mesh denser near the wall to capture the boundary layers.

Five different mesh types were considered where the number of divisions at the inlet were varied from 10 to 50 divisions as presented in Table 3 and for each case outlet average temperature was recorded while keeping an eye towards the convergence iteration. At the same time, the difference

between two consecutive iterations was calculated. Figure 4 shows the variation of pipe outlet temperature as element numbers increase due to increase in division.

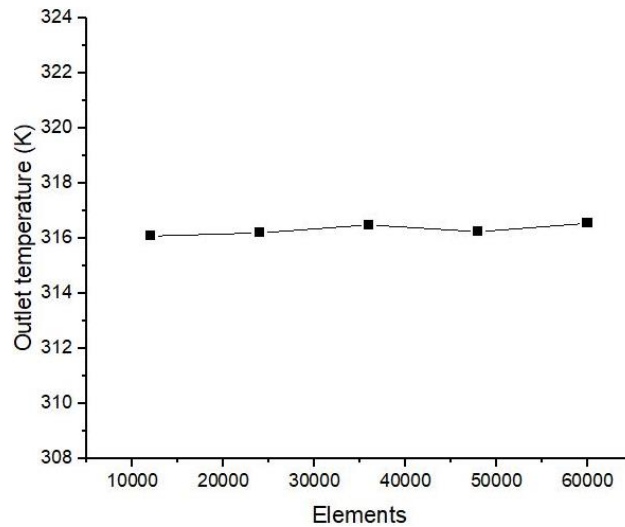


Fig. 4. Mesh Independence Study (MIS)

As seen on Table 3, the difference between mesh type 2 and mesh type 3 was comparatively higher. The difference went down for mesh type 4 and then increased again a little for mesh type 5. This is noticeable that the differences between outlet temperatures for the mesh types were very insignificant. It can be observed that, the iteration for convergence was the highest in mesh type 1. After that it suddenly dropped remarkably and started showing decent increase as divisions were increasing. Considering the differences in outlet temperature and the fact that higher iteration for convergence increases computational time, mesh type 4 was considered as the optimal mesh and all the simulations were run using this mesh type which contains 49241 nodes and 48000 elements. For the optimal mesh, the skewness and mesh quality were tested. The maximum and average skewness for this mesh was  $1.3253 \times 10^{-10}$  and  $1.3061 \times 10^{-10}$  respectively with an aspect ratio of 3.54781 which are within limits [23]. The orthogonal quality of the mesh is 1.00 which indicates the best orthogonal meshing. The difference in results between two consecutive mesh has been calculated using following formula:

$$\text{Percentage Difference} = \frac{| \text{Final Temperature} - \text{Initial Temperature} |}{\text{Initial Temperature}} * 100 \quad (8)$$

**Table 3**  
 Mesh Independence Study (MIS)

Mesh Type	Divisions	Nodes	Elements	Iteration for Convergence	Outlet average temperature (K)	Difference (%)
1	10	13211	12000	474	316.08	-
2	20	25221	24000	366	316.20	0.0379
3	30	37231	36000	360	316.49	0.0917
4	40	49241	48000	380	316.24	0.0789
5	50	61252	60000	393	316.55	0.0980

## 7. Validation

The Mixture model was validated by comparing with the experimental result of Pak and Cho [24] which has also been presented in benchmark research paper Bianco *et al.*, [21]. The same boundary conditions as the benchmark paper such as specified inlet and wall temperature were used to carry out the results. The validation has been done by examining the change in Nusselt number with Reynolds number ranging from 20000 to 80000 for 4% particle concentration. Reynolds number and Nusselt number has been calculated using following equations:

$$Re = \frac{\rho V D}{\mu} \quad (9)$$

$$Nu = \frac{h D}{k} \quad (10)$$

Here  $V$ ,  $h$  and  $D$  express flow velocity at fully developed region, heat flux and pipe diameter. The graph in Figure 5 represents the comparison between simulated and experimental  $Re$  vs  $Nu$  for Mixture model for particle concentration of 4% where the error from experimental result ranges from 11 to 15 percent. The average error shown by Mixture model for 4 different Reynolds numbers is 12.37%.

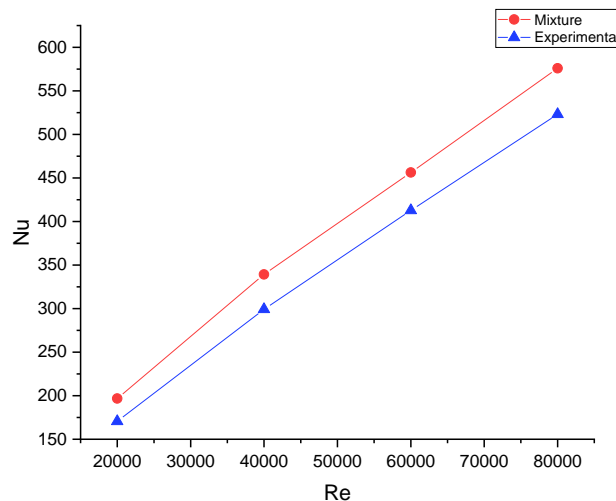


Fig. 5.  $Re$  vs  $Nu$  for particle concentration of 4%

## 8. Results and Discussion

Particle concentration is the key variable that dominates nanofluids heat transfer [25]. Having a look at how other variable reacts with the variation of particle concentration is essential. To understand the correlations well, first the Reynolds number was kept fixed at 40000 and the relationships between particle concentration and other variables were plotted accordingly.

Prandtl number is a variable that represents the ratio of momentum diffusivity to thermal diffusivity of forced convective heat transfer. With the increase in nanoparticle volume concentration from 1% to 6% the Prandtl number increases from 7.29 to 10.54 as seen in Figure 6. This indicates that as the particle volume concentration increases, the momentum diffusion becomes more dominant comparing to thermal diffusion. Meanwhile,  $St$  is a dimensionless number that measures the ratio between heat transfer into a fluid and the thermal capacity of the fluid. Perhaps it is called the dimensionless heat transfer coefficient. From Figure 7, it can be seen that as particle



concentration moves from 1% to 4% the increase in *St* is quite steep which is followed by a comparatively lower steep line to 6%. In fact, for increase in particle concentration by 3% from 1% to 4%, the Stanton number increases by 53.28%. This verifies that with the increase in solid particles in nanofluid the temperature difference from inlet to outlet per unit area goes significantly up. In other words, it indicates more heat transfer for more particles in nanofluids. Prandtl number and Stanton number have been calculated as following:

$$Pr = \frac{\mu C_p}{k} \tag{11}$$

$$St = \frac{h}{\rho \mu C_p} \tag{12}$$

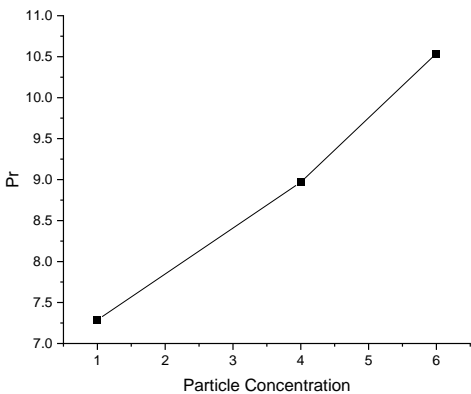


**Fig. 6.** Particle concentration vs Prandtl Number

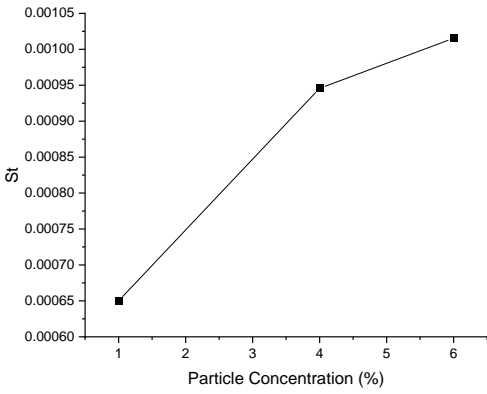


**Fig. 7.** Particle concentration vs Stanton Number

The next important variable is Peclet number (*Pe*). Peclet number represents the ratio between advective transport rate vs mass diffusion rate. Figure 8 represents the increase in *Pe* as particle concentration is increased from 1% to 6%. It can be seen that as particle concentration keeps increasing *Pe* increases dramatically. For *Re* 40000 as particle concentration increases from 1% to 6% *Pe* goes up from 290000 to 420000. This indicates, as particle concentration increases in nanofluid, heat transfer in nanofluid becomes more advection dominant and less diffusion dominant. Thermal Entry Length (TEL) represents the distance from the inlet of the pipe where the temperature profile inside the pipe becomes stable and reaches the steady state. As presented in Figure 9, with the increase in particle concentration, TEL follows the same trend as *Pe*. For 3% increase in particle concentration, the thermal entry length increases by almost 23.05% whereas for further 2% particle concentration increment it increases about 17.5%. *Pe* and TEL have been calculated as following:

$$Pe = \frac{u \rho C_p L}{k} \tag{13}$$

$$TEL = 0.05 Re Pr D \tag{14}$$

Where, *u*, *C<sub>p</sub>*, *L*, *K* and *D* represent flow velocity, specific heat, characteristic length, thermal conductivity and pipe diameter respectively.

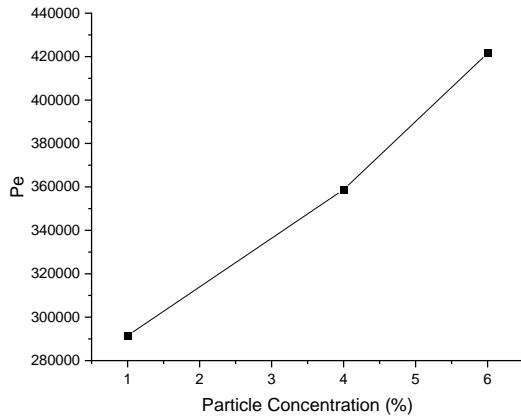


**Fig. 8.** Particle concentration vs Peclet Number

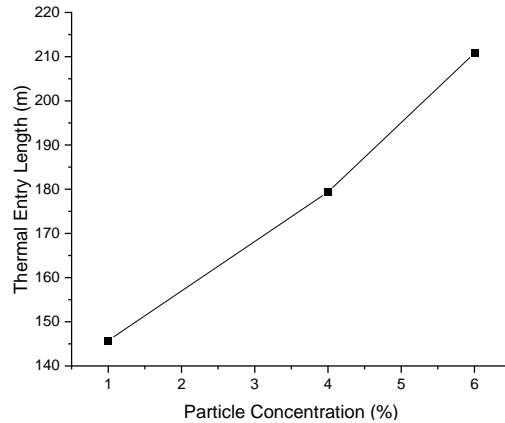


**Fig. 9.** Particle concentration vs Thermal Entry Length

One of the most important variables in convective heat transfer that tells how fast heat is being transferred by a fluid via convection than conduction is the Nusselt number which is represented by Eq. (8). Nu is a function of the convective heat transfer coefficient and as seen from Figure 10 and Figure 11, the heat transfer coefficient and Nu both rises significantly as particle concentration increases for a certain Re. In fact, as particle concentration is raised from 1% to 6%, Nu increases from 260.32 to 330.7 (27.04%). So, this is quite transparent that for a fixed Re, the heat transfer by nanofluids is dominated by the amount of nanoparticle present in the fluid.

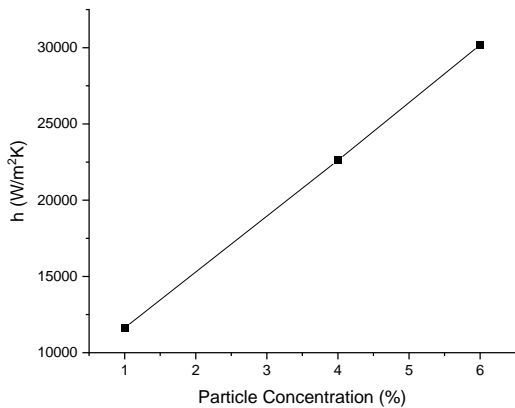


**Fig. 10.** Particle concentration vs heat transfer coefficient

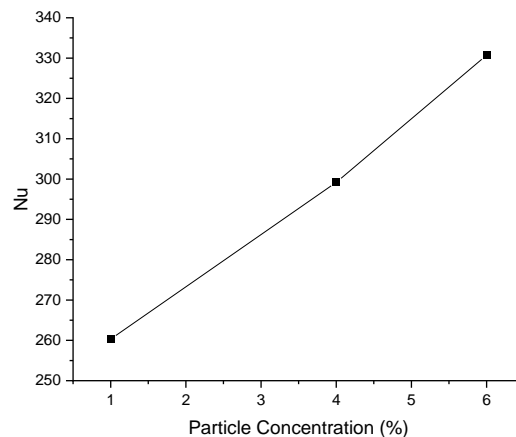


**Fig. 11.** Particle concentration vs Nusselt number

The variable considered next is skin friction factor. This gives idea about local dynamic pressure and shear stress on the wall. For Re 40000 the particle concentration was increased from 1% to 4%. It was observed that the skin friction decreases by a negligible amount (see Figure 12). For increase of 5% in particle concentration the decrease in skin friction coefficient is 0.0006. This takes us to the relationship between particle concentration and wall shear stress on the pipe (see Figure 13). Though the skin friction coefficient seems to decrease by a very small amount wall shear stress increases as concentration goes high. For a fixed Re of 40000 as particle concentration goes up from 1% to 6%, wall shear stress increases from 46.54 Pa to 98.98 Pa.

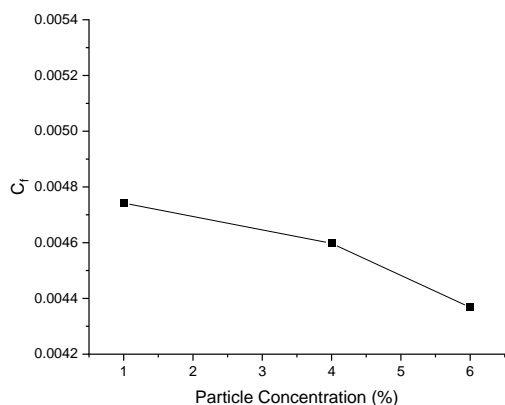


**Fig. 12.** Particle concentration vs skin friction coefficient

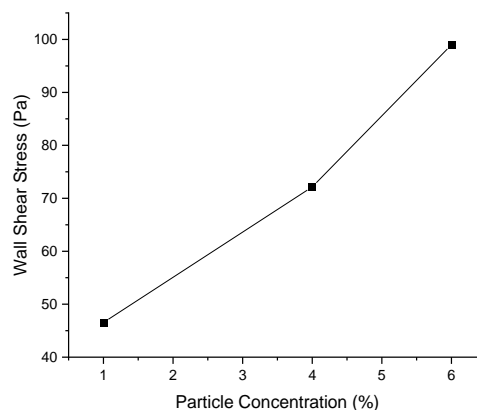


**Fig. 13.** Particle concentration vs wall shear stress

A question of anomaly might rise because the skin friction coefficient remains almost unchanged, but wall friction factor increases. This is because the wall shear stress is dependent on two other variables other than the friction factor which are density and the square of velocity. This is quite apparent that wall shear stress is more dominated by density and velocity than by friction coefficient. As nanoparticle concentration increases the density of nanofluid increases significantly, to maintain the same Re velocity has to increase. Consequently, as nanoparticle concentration increases, the wall shear stress rises dramatically.

For the subsequent correlations, particle concentration was kept fixed at 4% and Re was varied from, 20000 to 80000 and it was observed how the variables react.

Firstly, Pe was deduced with respect to Re. As seen from Figure 14, Pe escalates linearly with hike in Re. This is because when the density and viscosity of a fluid is constant, Re depends on flow velocity and as flow velocity goes up the degree of advection increases which is indicated by Pe. Further, it is observed from Figure 15, as Pe grows, Nu goes up linearly. This validates that as the nanofluid flow becomes more advection dominant, the heat transfer tendency via convection keeps increasing.

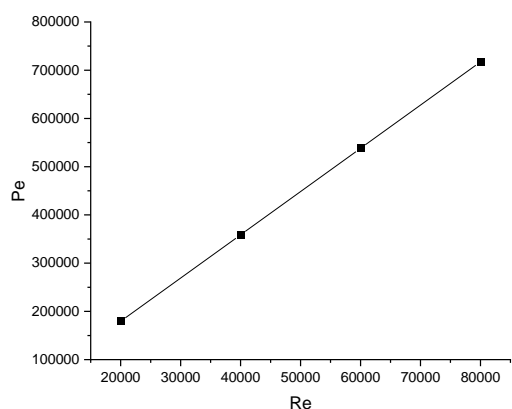


**Fig. 14.** Reynolds Number vs Peclet number

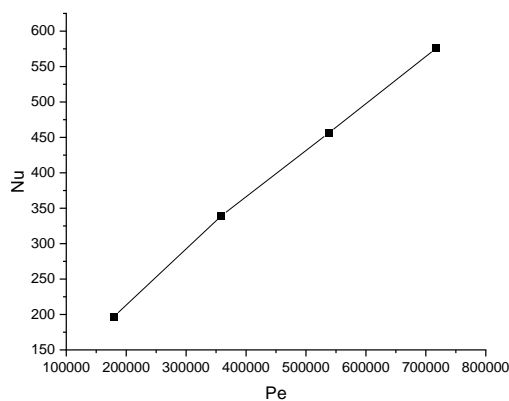


**Fig. 15.** Peclet Number vs Nusselt number

Figure 16 represents the relationship between Re and St while particle concentration is kept fixed at 4%. As Re goes high St seem to decrease almost linearly with a bit of fluctuation. That means St is inversely proportional to Re. The significance of this information is, as velocity of nanofluid flow increases the temperature difference between inlet and outlet per unit area goes down though the heat transfer rate increases because mass flow rate raises with velocity. For volume concentration of 4 percent, relationship between Re and Nu has been established as depicted in Figure 17. As Re goes from 20000 from 80000 the Nu increases from 196.77 which depicts the proportional relationship

between Re and Nu for fixed particle concentration of nanofluid. The point to be noted is that, as Re is increased from 20000 to 40000, Nu increases by 72.42%, whereas for hike in Re from 60000 to 80000, Nu increases by 26.21%, Which means, even for turbulent convective heat transfer of nanofluids, the rate of heat transfer enhancement is comparatively slower at the higher degree of turbulence.

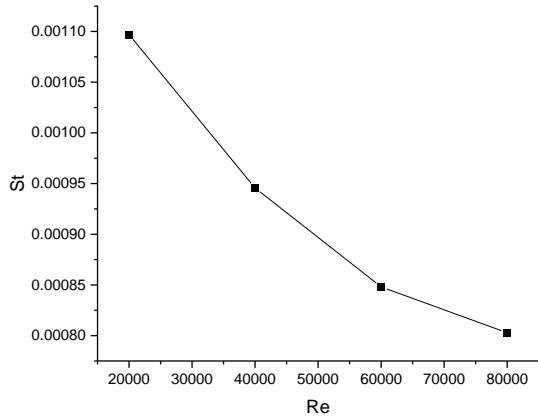


Fig. 16. Reynolds number vs Stanton number

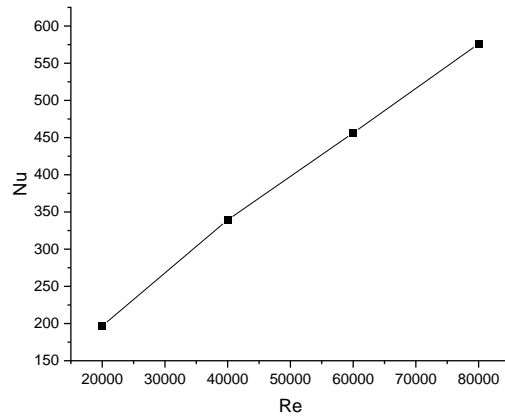


Fig. 17. Reynolds number vs Nusselt number

The effect of boundary condition on heat transfer has been examined by varying the wall temperature and the inlet temperature. First inlet temperature was kept constant at 293 K and heat transfer coefficient and Nusselt number was plotted against wall temperature of 300 K, 350 K and 400 K as presented in Figure 18 and Figure 19. The heat transfer coefficient and Nu remains almost the same for varied wall temperature.

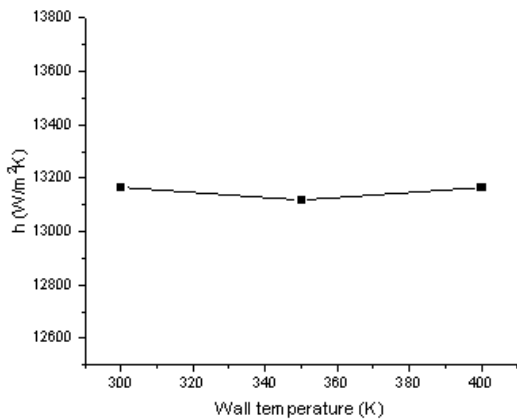


Fig. 18. Wall temperature vs heat transfer coefficient

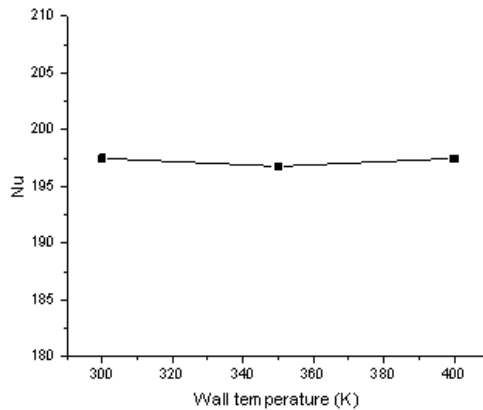
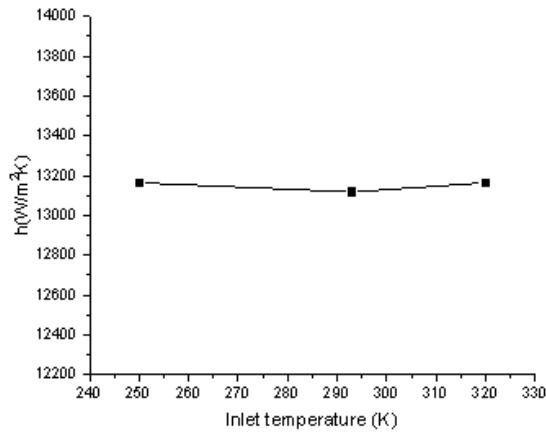


Fig. 19. Wall temperature vs Nusselt number

After that wall temperature was kept constant at 350 K and heat transfer coefficient and Nusselt number were calculated for inlet temperature of 250 K, 293 K and 320 K as presented in Figure 20 and Figure 21. It is seen that the heat transfer coefficient and Nu follows the same trend as they did for variable wall temperature. This is because, as inlet and wall temperatures are increased, the logarithmic mean temperature difference adjusts itself in a way that the amount of heat transfer enhancement is the same. This is logical because, nanofluids heat transfer is dominated by Re and Particle concentration. Any boundary condition can only affect the outlet temperature. But the heat transfer enhancement stays the same for a certain particle concentration at a certain Re. The little

deflection at the mid-point is probably because of rounding up the values and time variant simulation power of the computer processor.



**Fig. 20.** Inlet temperature vs heat transfer coefficient

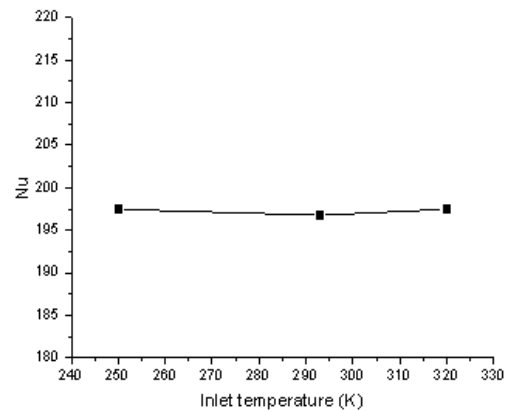


**Fig. 21.** Inlet temperature vs Nusselt number

Finally, particle concentration was kept constant at 4% with Re constant at 40000 and particle size was varied from 10 nm to 40 nm to see how this affects the transfer of heat. The heat transfer investigation was carried out by examining two variables: outlet temperature and Nu.

It was seen that according to mixture model, as particle size changes from 10 nm to 40 nm there is no change in outlet temperature and Nu at all as seen in Figure 22 and Figure 23.

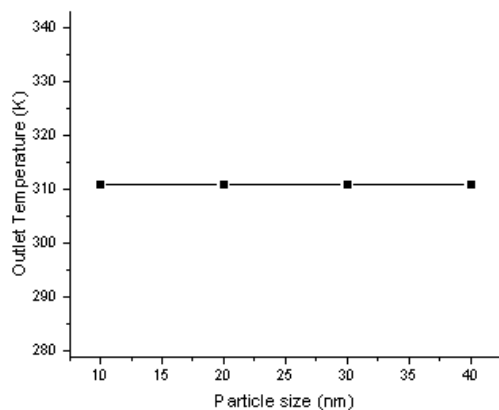


**Fig. 22.** Particle size vs Outlet temperature

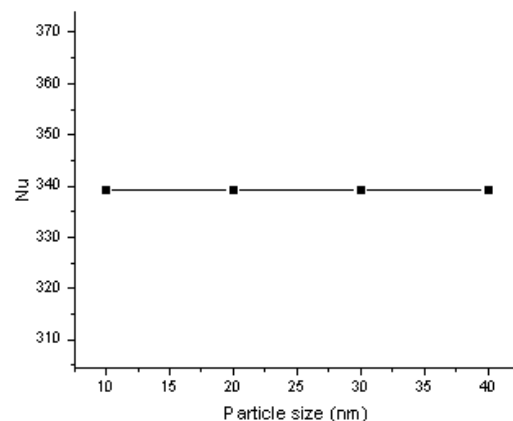


**Fig. 23.** Particle size vs Nusselt number

When skin friction factor and wall shear stress was drawn against particle size as Figure 24 and Figure 25, they followed same trend as outlet temperature and Nu.

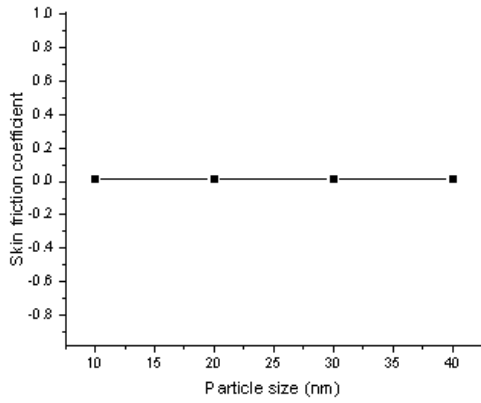


**Fig. 24.** Particle size vs Skin friction coefficient

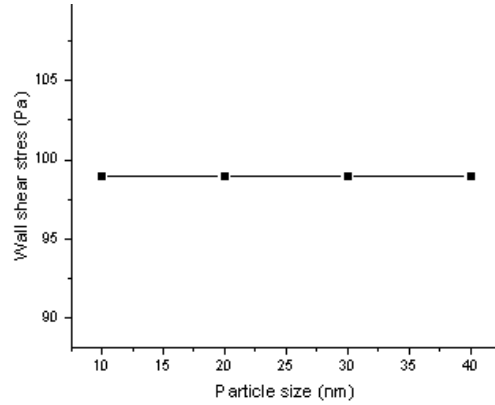
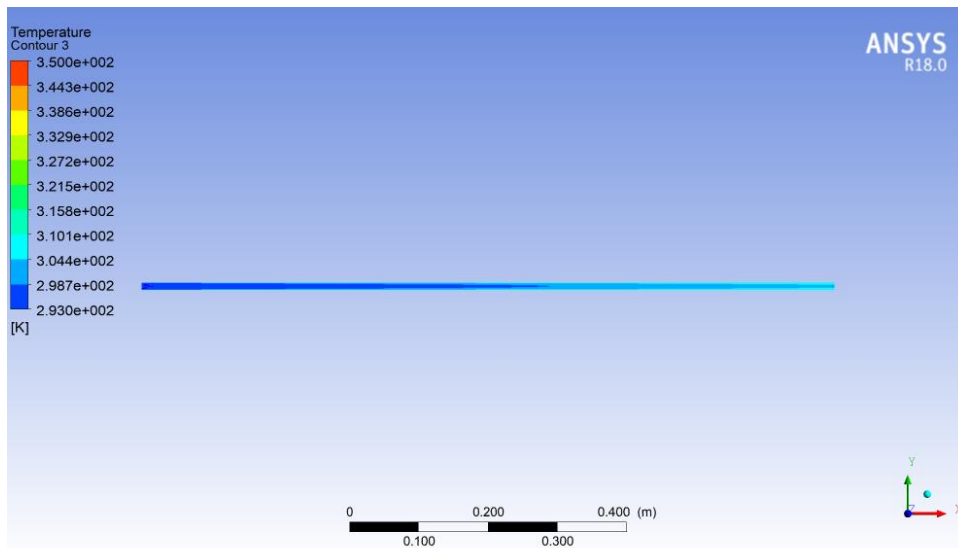


**Fig. 25.** Particle size vs Wall shear stress

This raises a bit of confusion. Because according to the experimental studies, variation in particle size does affect the heat transfer. But according to the simulated results not only the transfer of heat remains the same, but also the local dynamic pressure and shear stress is unchanged. So, this can be said that Mixture model is not able to assess the effect of nanoparticle size variation on heat transfer of nanofluids. This is because the mixture model takes the overall density of nanofluid into account regardless particle size. And for a certain concentration the density is fixed. So, the heat transfer coefficient, Nusselt number, wall shear stress and skin friction coefficient are also predicted to be fixed by this model.

Figure 26 shows temperature contours by Mixture model when Re is kept fixed at 40000 and particle concentration is varied from 1% to 4%.



(a)

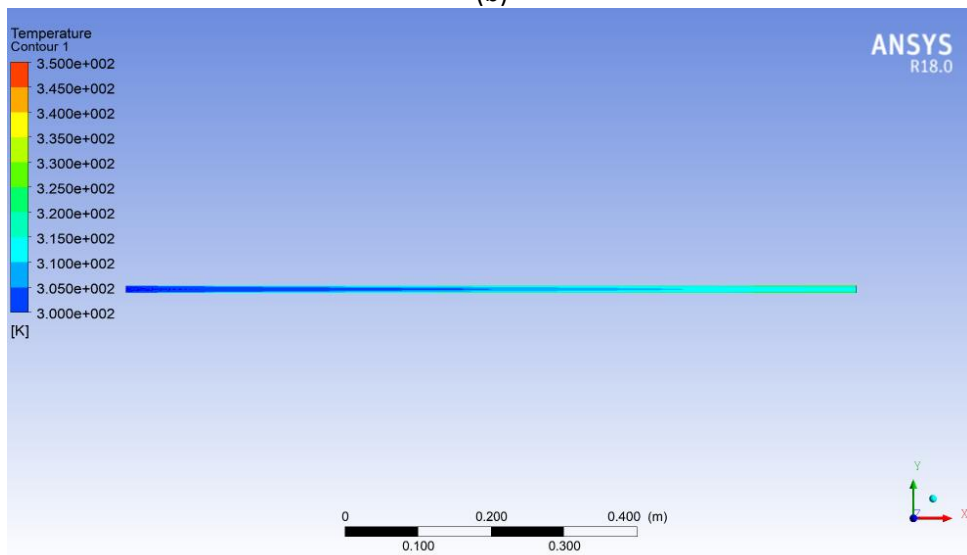
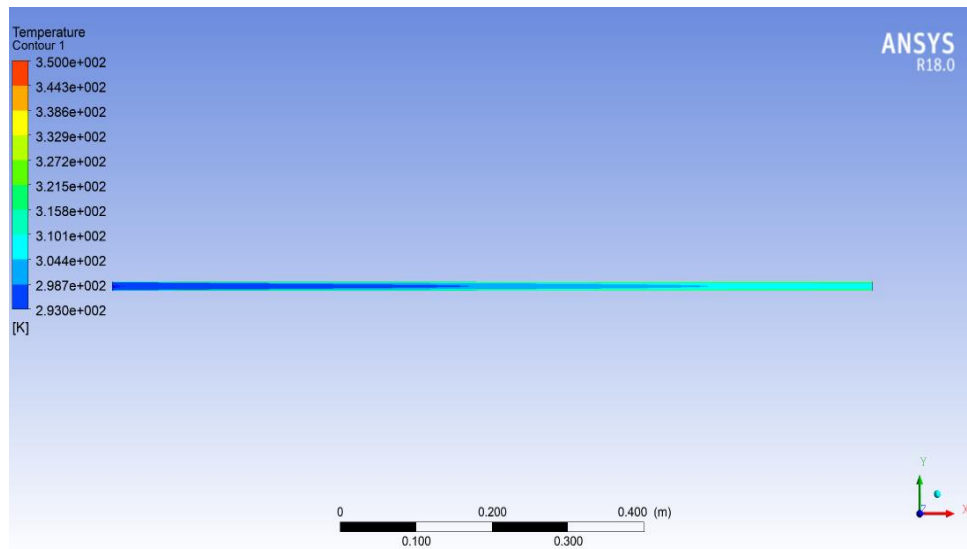


**Fig. 26.** Temperature contour for Re 40000 for particle concentration of (a) 1%, (b) 4% and (c) 6% for Mixture model

## 9. Conclusion

- I. The turbulent convective heat transfer of nanofluids is mostly dominated by particle concentration. When the particle concentration is fixed the transfer of heat depends on the degree of turbulence. Prandtl number, Stanton number, Peclet number, Thermal Entry Length, Nusselt number and wall shear stress are directly proportional to nanoparticle particle concentration of nanofluid whereas the skin friction coefficient is inversely proportional to it. Though for a fixed particle concentration, Nusselt number and Peclet number behaves proportionally with Reynolds number, Stanton number is inversely proportional to Reynolds number.
- II. The heat transfer enhancement of nanofluids is independent of temperature boundary conditions.

- III. The Mixture model is unable to investigate the effect of particle size variation on heat transfer enhancement of nanofluids when smaller nanoparticles are used. Some further experimental and also CFD investigation can be done using Mixture model with comparatively bigger particles to see if it behaves differently.

### Acknowledgement

This research was not funded by any grant.

### References

- [1] Sreelakshmy, K. R., Aswathy S. Nair, K. Vidhya, T. Saranya, and Sreeja C. Nair. "An overview of recent nanofluid research." *International Research Journal of Pharmacy* 5, no. 4 (2014): 239-243. <https://doi.org/10.7897/2230-8407.050451>
- [2] Hanafizadeh, P., M. Ashjaee, M. Goharkhah, K. Montazeri, and M. Akram. "The comparative study of single and two-phase models for magnetite nanofluid forced convection in a tube." *International Communications in Heat and Mass Transfer* 65 (2015): 58-70. <https://doi.org/10.1016/j.icheatmasstransfer.2015.04.012>
- [3] Lotfi, R., Y. Saboohi, and A. M. Rashidi. "Numerical study of forced convective heat transfer of nanofluids: comparison of different approaches." *International Communications in Heat and Mass Transfer* 37, no. 1 (2010): 74-78. <https://doi.org/10.1016/j.icheatmasstransfer.2009.07.013>
- [4] Davarnejad, Reza, and Maryam Jamshidzadeh. "CFD modeling of heat transfer performance of MgO-water nanofluid under turbulent flow." *Engineering Science and Technology, an International Journal* 18, no. 4 (2015): 536-542. <https://doi.org/10.1016/j.jestch.2015.03.011>
- [5] Fard, M. Haghshenas, M. Nasr Esfahany, and M. R. Talaie. "Numerical study of convective heat transfer of nanofluids in a circular tube two-phase model versus single-phase model." *International Communications in Heat and Mass Transfer* 37, no. 1 (2010): 91-97. <https://doi.org/10.1016/j.icheatmasstransfer.2009.08.003>
- [6] Kriby, Saliha, Mohamed Announ, and Tayeb Kermezi. "2D CFD simulation to investigate the thermal and hydrodynamic behavior of nanofluid flowing through a pipe in turbulent conditions." *CFD Letters* 11, no. 11 (2019): 58-75.
- [7] Bianco, Vincenzo, Oronzio Manca, and Sergio Nardini. "Numerical investigation on nanofluids turbulent convection heat transfer inside a circular tube." *International Journal of Thermal Sciences* 50, no. 3 (2011): 341-349. <https://doi.org/10.1016/j.ijthermalsci.2010.03.008>
- [8] Esfandiary, M., A. Habibzadeh, and H. Sayehvand. "Numerical Study of Single Phase/Two-Phase Models for Nanofluid Forced Convection and Pressure Drop in a Turbulence Pipe Flow." *Trans. Phenom. Nano Micro Scales* 4, no. 1 (2016): 11-18.
- [9] Akbari, Omid Ali, Mohammad Reza Safaei, Marjan Goodarzi, Noreen Sher Akbar, Majid Zarringhalam, Gholamreza Ahmadi Sheikh Shabani, and Mahidzal Dahari. "A modified two-phase mixture model of nanofluid flow and heat transfer in a 3-D curved microtube." *Advanced Powder Technology* 27, no. 5 (2016): 2175-2185. <https://doi.org/10.1016/j.apt.2016.08.002>
- [10] Amani, Mohammad, Pouria Amani, Alibakhsh Kasaeian, Omid Mahian, and Wei-Mon Yan. "Two-phase mixture model for nanofluid turbulent flow and heat transfer: Effect of heterogeneous distribution of nanoparticles." *Chemical Engineering Science* 167 (2017): 135-144. <https://doi.org/10.1016/j.ces.2017.03.065>
- [11] Hussein, Adnan M., R. A. Bakar, and K. Kadrigama. "Study of forced convection nanofluid heat transfer in the automotive cooling system." *Case Studies in Thermal Engineering* 2 (2014): 50-61. <https://doi.org/10.1016/j.csite.2013.12.001>
- [12] Parvin, S., R. Nasrin, M. A. Alim, and N. F. Hossain. "Effect of Prandtl number on forced convection in a two sided open enclosure using nanofluid." *Journal of Scientific Research* 5, no. 1 (2013): 67-75. <https://doi.org/10.3329/jsr.v5i1.9641>
- [13] Anoop, K. B., T. Sundararajan, and Sarit K. Das. "Effect of particle size on the convective heat transfer in nanofluid in the developing region." *International Journal of Heat and Mass Transfer* 52, no. 9-10 (2009): 2189-2195. <https://doi.org/10.1016/j.ijheatmasstransfer.2007.11.063>
- [14] Zhang, Liang, Anlong Zhang, Yuyan Jing, Pingping Qu, and Zhaoran Wu. "Effect of Particle Size on the Heat Transfer Performance of SiO<sub>2</sub>-Water Nanofluids." *The Journal of Physical Chemistry C* 125, no. 24 (2021): 13590-13600. <https://doi.org/10.1021/acs.jpcc.1c02014>
- [15] Angayarkanni, S. A., Vijutha Sunny, and John Philip. "Effect of nanoparticle size, morphology and concentration on specific heat capacity and thermal conductivity of nanofluids." *Journal of Nanofluids* 4, no. 3 (2015): 302-309. <https://doi.org/10.1166/jon.2015.1167>



- [16] Khatke, Vivekanand Limbaji, Manil Rathi, V. L. Bhanavase, and A. J. Patil. "Effect of nanoparticle size on heat transfer intensification." In *International Conference on Ideas, Impact and Innovation in Mechanical Engineering*, vol. 5, no. 6, pp. 520-526. 2017.
- [17] Du, Ruiqing, Dandan Jiang, and Yong Wang. "Numerical investigation of the effect of nanoparticle diameter and sphericity on the thermal performance of geothermal heat exchanger using nanofluid as heat transfer fluid." *Energies* 13, no. 7 (2020): 1653. <https://doi.org/10.3390/en13071653>
- [18] Azimi, Seyyed Shahabeddin, Mansour Kalbasi, and Mohammad Hosain Namazi. "Effect of nanoparticle diameter on the forced convective heat transfer of nanofluid (water+ Al<sub>2</sub>O<sub>3</sub>) in the fully developed laminar region." *International Journal of Modeling, Simulation, and Scientific Computing* 5, no. 03 (2014): 1450008. <https://doi.org/10.1142/S1793962314500081>
- [19] Davarnejad, Reza, Sara Barati, and Maryam Kooshki. "CFD simulation of the effect of particle size on the nanofluids convective heat transfer in the developed region in a circular tube." *SpringerPlus* 2, no. 1 (2013): 1-6. <https://doi.org/10.1186/2193-1801-2-192>
- [20] Al Mahmud, Suaib, and Ahmad Faris Ismail. "Multiphase CFD Investigation on Convective Heat Transfer Enhancement for Turbulent Flow of Water-Al<sub>2</sub>O<sub>3</sub> Nanofluid." *CFD Letters* 13, no. 10 (2021): 11-24. <https://doi.org/10.37934/cfdl.13.10.1124>
- [21] Bianco, Vincenzo, Oronzio Manca, and Sergio Nardini. "Numerical simulation of water/Al<sub>2</sub>O<sub>3</sub> nanofluid turbulent convection." *Advances in Mechanical Engineering* 2 (2010): 976254. <https://doi.org/10.1155/2010/976254>
- [22] ANSYS, Inc. "ANSYS fluent theory guide (release 13.0)." ANSYS, Canonsburg, PA (2013).
- [23] Alawadhi, Esam M. "Meshing guide." In *Finite Element Simulations Using ANSYS*, pp. 407-424. CRC Press, 2015. <https://doi.org/10.1201/b18949-12>
- [24] Pak, Bock Choon, and Young I. Cho. "Hydrodynamic and heat transfer study of dispersed fluids with submicron metallic oxide particles." *Experimental Heat Transfer an International Journal* 11, no. 2 (1998): 151-170. <https://doi.org/10.1080/08916159808946559>
- [25] Mousavi, S. M., F. Esmaeilzadeh, and X. P. Wang. "Effects of temperature and particles volume concentration on the thermophysical properties and the rheological behavior of CuO/MgO/TiO<sub>2</sub> aqueous ternary hybrid nanofluid." *Journal of Thermal Analysis and Calorimetry* 137, no. 3 (2019): 879-901. <https://doi.org/10.1007/s10973-019-08006-0>